An introduction to electrical resistivity in geophysics

Rhett Herman[a)]
Department of Chemistry and Physics and Department of Geology, Radford University, Radford, Virginia 24142

(Received 7 July 2000; accepted 22 March 2001)

Physicists are finding that the skills they have learned in their training may be applied to areas beyond traditional physics topics. One such field is that of geophysics. This paper presents the electrical resistivity component of an undergraduate geophysics course at Radford University. It is taught from a physics perspective, yet the application of the theory to the real world is the overriding goal. The concepts involved in electrical resistivity studies are first discussed in a general sense, and then they are studied through the application of the relevant electromagnetic theory. Since geology majors comprise the bulk of the students in this class, the math used is only that which is typically required of geology majors. The final results are given in a form that practicing geophysicists may use in the field. A method is presented for constructing an inexpensive apparatus for measuring electrical resistivity in both a tabletop laboratory setting and in the field. This apparatus is truly ''plug and play'' since its assembly and use requires only the most basic knowledge of electronics. This apparatus is tested in a tabletop laboratory setting as well as in two field surveys.
[DOI: 10.1119/1.1378013]

I. INTRODUCTION

Introductory physics courses are typically survey courses introducing students to a large number of topics in one year. The laboratory sessions that accompany these courses are usually designed to illustrate a very specific concept, using tabletop equipment designed specifically for that lab. These types of labs, while necessary to focus the students' attention on a particular new concept, are often viewed as inapplicable to the real world due to their very focused nature.[1] Upper-level applied physics courses are often the first place where students move from studying theory in ideal situations to the application of that theory to real-world circumstances. These applied physics courses take many different ideas in physics—often very diverse ideas—and apply them to the study of a particular problem. The cross-disciplinary field of geophysics provides a venue for many such applications of physics theories to real-world situations.

A course in geophysics should appeal to geology majors as well as physics majors. Geology majors will have expectations of such a course that are different from the expectations of physics students.[2–5] Physics students are used to seeing coverage of topics starting from first principles and proceeding via the tools of math until a final equation is achieved. These physics students then typically practice the use of that equation by working as many problems using that equation as possible. Geology students are quite eager to study the concepts and visualize real-world situations, and, in the end, trust that the final mathematical answer has been derived once by others and need not be rederived for their edification. While physics students are often content to stop once the final equation is achieved, geology students are much more desirous of seeing how the final equation applies to as wide a variety of actual field situations as possible. A course in geophysics can meet the needs of both of these populations by starting with the concepts, performing the required mathematical derivations, and then showing the application of the mathematical results to the physical world outside of the ideal classroom or laboratory setting.

In this paper, the electrical resistivity section of a course in geophysics taught at Radford University is described. The application of the techniques of physics to the study of field geophysics yields a natural arena wherein several of the basic concepts of physics may be integrated into a single area of study. Several topics in electromagnetic theory are illuminated in this study including the vector form of Ohm's law, the nature of the current density vector $\mathbf{J}$, the nature of electrical resistivity and its inverse electrical conductivity, and the difference between the electric potential and the electric field.

As an advanced applied physics course, the accompanying lab needs to illustrate the application of the theory to settings beyond the typical tabletop experiment. Geologists especially need to do experiments out-of-doors in the nonideal settings they will encounter in their professional lives. The equipment the students use must be capable of taking data comparable to that which the students would encounter were they to go into geophysics professionally. As at many institutions, the budget for this equipment was limited. Yet it was this budgetary limitation that became the impetus for constructing equipment for the resistivity lab that would ultimately serve students' educational needs better than purchasing commercial resistivity equipment.

A section of a geophysics course studying electrical resistivity has recently been described in this journal.[6] There are two main differences between that work and the present. The first of these is the reliance in this paper on more elementary calculations. This is done since geology majors typically have less experience and comfort with math beyond first-year calculus than physics majors. This results in a trade-off of the more mathematical approach of Avants *et al.*[6] in favor of the more conceptual approach described here. The present work starts from the vector form of Ohm's law $\mathbf{J}=\sigma\mathbf{E}$, and proceeds through a first-order rather than a second-order differential equation. The second major difference is that the components of the equipment described in this paper may be

purchased from typical retail electronics and hardware stores and require the user to simply ''plug and play'' the individual components in order to obtain the data.

Equipment purchased from commercial vendors for a geophysics laboratory is quite expensive. Typical field setups for electrical resistivity studies have prices starting at $20,000 and rising from that number, depending on the complexity of the equipment. Much of this cost is due to the fact that commercial equipment takes, stores, and analyzes the hundreds of data points required for a commercial survey. If this equipment were to be used by students unfamiliar with its inner workings, then it would become a ''black box'' situation where the students record the numbers the equipment gives them without having physical intuition about how the equipment obtained the readings. In addition, the software that typically accompanies commercial equipment performs the data analysis required to build a picture of the subsurface structure without any human involvement. While this is ideal for field geophysicists operating under time constraints, it again makes for a black box situation when students are first learning how the individual data points are used to build that final picture of the subsurface structure.

The apparatus described here addresses both the issue of cost and the issue of the possible black box nature of the laboratory equipment. The resistivity apparatus is constructed from off-the-shelf components available from typical retail electronics and hardware stores. The total cost of the components described in this paper was under $350. The components are connected in a visible manner such that the students are able to see how the entire apparatus works to acquire each data point. This apparatus may be assembled with only the most basic knowledge of electronics.

Section II presents a conceptual introduction to the electromagnetic theory pertinent to the study of the electrical resistivity method of field geophysics. The concepts presented allow students to visualize the flow of current through various subsurface layers and how that flow is affected by the resistivities of the different layers. Qualitative explanations are presented as to how simple measurements of voltage and current obtained at the surface yield information about the composition of the underlying materials. Section III presents the mathematical formulation of the theory. This formulation begins with the vector form of Ohm's law and proceeds via the solution of a first-order differential equation rather than a second-order differential equation. The equations relevant to an introduction to electrical resistivity studies in geophysics are derived and related to the qualitative discussions of Sec. II. These equations may then be used to process field data in order to reveal the subsurface structure of the survey area. Section IV describes an inexpensive apparatus that may be constructed with commercially available components. Section V presents the results of using the equipment described in Sec. IV to acquire resistivity data in both laboratory and field settings.

II. RESISTIVITY THEORY: CONCEPTUAL INTRODUCTION

Electrical resistivity studies in geophysics may be understood in the context of current flow through a subsurface medium consisting of layers of materials with different individual resistivities.[7–10] For simplicity, all layers are assumed to be horizontal. The resistivity ρ of a material is a measure of how well the material retards the flow of electrical current.

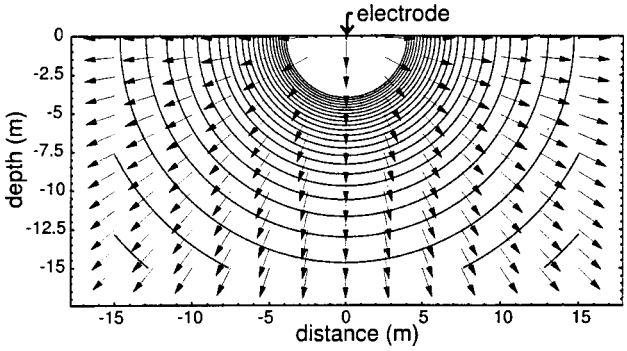

Fig. 1. Current flow and equipotential surfaces in a level field with homogeneous subsurface structure. The unit vector field shows the directions of the current density **J** and thus the electric field **E**.

Resistivities vary tremendously from one material to another. For example, the resistivity of a good conductor such as copper is on the order of $10^{-8}\,\Omega$ m, the resistivity of an intermediate conductor such as wet topsoil is $\sim 10\,\Omega$ m, and the resistivity of poor conductors such as sandstone is $\sim 10^{8}\,\Omega$ m. Due to this great variation, measuring the resistivity of an unknown material has the potential for being very useful in identifying that material, given little further information. In field studies, the resistivity of a material may be combined with reasoning along geologic lines to identify the materials that constitute the various underground layers.

Resistivity is often first encountered in physics when discussing the resistance of an ideal cylinder of length L and cross-sectional area $\boldsymbol{A}$ of uniform composition. The resistivity ρ appears as the material-specific constant of proportionality in the expression for the total resistance of the cylinder,

$$\boldsymbol{R}=\rho\frac{\boldsymbol{L}}{\boldsymbol{A}}. \tag{1}$$

The total resistance R may be obtained experimentally through Ohm's law, $\boldsymbol{R}=\boldsymbol{V}/\boldsymbol{I}$, where V is the potential difference between the ends of the cylinder and I is the total current flowing through the cylinder. Edge effects are not considered. The resistivity of the material, an intrinsic property of the material, is then related to experimentally measured extrinsic parameters by

$$\rho=\left(\frac{V}{I}\right)\left(\frac{A}{L}\right)=\boldsymbol{R}_{\mathrm{app}}\boldsymbol{K}. \tag{2}$$

In Eq. (2), the resistivity is given by the product of the ''apparent resistance'' $\boldsymbol{R}_{\mathrm{app}}=(\boldsymbol{V}/\boldsymbol{I})$ and a ''geometric factor'' $\boldsymbol{K}=(\boldsymbol{A}/\boldsymbol{L})$ that carries information about the geometry of the cylinder. This type of product of an apparent resistance and a geometric factor will appear again when the resistivity of the ground is determined.

It is more difficult to arrive at an expression for the resistivity of material that is not as geometrically simple as a uniform cylinder. A good starting point is shown in Fig. 1, which depicts current flowing radially away from a single electrode at positive potential located on the surface of the ground. The subsurface is of uniform composition, and $V=0$ infinitely far away from the electrode. Equipotential surfaces are indicated by solid lines, while the unit vector field shows the direction of **J** and thus **E**. The equipotential surfaces are perpendicular to the lines of current and may be understood as creating the local potential gradients or ''volt-

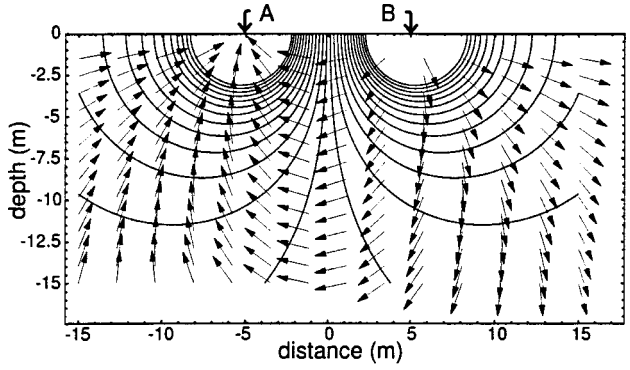

Fig. 2. Current flow and equipotential surfaces between the two current electrodes ***A*** and ***B*** in a level field with homogeneous subsurface structure.

age drops'' that drive the current according to the simple scalar form of Ohm's law given by $I=V/R$. The resistance of the air above the ground is assumed to be infinite so that the ground forms a Dirichlet-type boundary.[11]

A more realistic situation is depicted in Fig. 2. The two current electrodes are labeled *A* and *B* by convention. Figure 2 shows the current in one ac cycle flowing from *B* to *A*, with each line of current being driven from higher to lower potential throughout the medium. A plane of symmetry exists at the midpoint between the electrodes. It should be noted that alternating current is used in these studies to avoid macroscopic polarization of the subsurface material.[10] Such macroscopic polarization would result from the bulk migration of charges in the subsurface in response to a constant applied field. This would create an artificial dc potential that would interfere with the resistivity measurements. An ac frequency in the range 1–100 Hz is sufficient to avoid this problem.[7–10]

Figure 2 indicates that the spacing of the two current electrodes will determine the ''effective depth'' to which the current will penetrate. If the spacing between ***A*** and ***B*** is on the order of a meter, then the vast majority of the total current will flow no more than a few meters from the surface. If the spacing between ***A*** and ***B*** is on the order of a kilometer, then most of the current will penetrate very deeply into the underlying material as it travels from *A* to *B*. Thus, the resistance that the current encounters between the electrodes is due primarily to the material that is at a depth that is less than several times the spacing of the current electrodes. For a uniform subsurface structure of Fig. 1, this is irrelevant since the entire subsurface would have the same resistivity. The effective depth does become relevant with the inhomogeneous subsurface shown in Fig. 3.

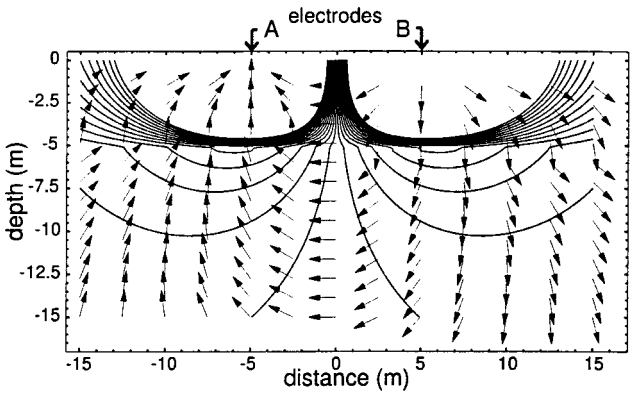

Fig. 3. Current flow and equipotential surfaces between two electrodes in a level field with inhomogeneous subsurface structure. The boundary between the two materials in this example is at a depth of $z=5$ m.

Figure 3 illustrates the current flow when the subsurface material contains an upper region with higher resistivity than the resistivity of the region below. When the current encounters the region of lesser resistivity, the equipotential surfaces are further apart, and the current will alter its course through the lower material accordingly. If the distance between the current electrodes is the same, then the total resistance the current encounters in the situation in Fig. 3 will be less than that depicted in Fig. 2. The total measured resistivity will be similarly lower, and the current will flow more easily between the electrodes. This alteration of the current flow between the electrodes is the basis for discerning both the presence of the boundary between the two layers as well as a value for the resistivity of the material in the lower layer.

Figure 3 indicates qualitatively how resistivity studies are able to discern the presence of the two layers. When the spacing between the current electrodes is much less than the depth of the boundary between the two layers, most of the current will not encounter the region of lower resistivity. This means that the total resistivity measured at the surface will be mostly due to the material that lies above the boundary. When the current electrodes are placed further apart, the current penetrates more and more into the region of lower resistivity, and the total resistivity begins to decrease from its initial value that it has when the electrodes are close together. When the spacing between the current electrodes is much greater than the depth of the boundary, most of the current will spend most of its journey in the region of lower resistivity. The overall resistivity measured at the surface will be mostly due to the material in the lower layer.

It should be noted here that the total resistivity measured at the ground surface in field studies of multilayer systems is not the true resistivity of the underlying material. The measured resistivity is a weighted average of the resistivities of the various materials that the current encounters.[8,9] When the current electrodes are placed very close together in the two-layer system of Fig. 3, some small amount of the current still penetrates to the deep layer. Thus, the measured resistivity will not be exactly that of the upper material. Similarly, when the electrodes are spaced very far apart, some of the current still traverses the upper layer. The overall resistivity measured at the surface will then only asymptotically approach that of the lower material as the electrodes are moved toward infinite separation.

The behavior of the apparent resistivity of such an ideal two-layer system is shown in Fig. 4, which plots the resistivity values $\{\rho_1,\rho_2,\ldots,\rho_N\}$ versus the ''effective depths'' $\{z_1,z_2,\ldots,z_N\}$ to which the current is probing the subsurface. The quantity N is the total number of data points collected. In the next section, the effective depth z will be related to the physical layout of the electrodes on the surface. Figure 4 shows the transition from the higher apparent resistivity of the upper layer to the lower apparent resistivity of the deeper layer.

Just as the resistivity values obtained at the surface are apparent resistivities and not the true resistivities of the underlying material, so too are the effective depths $\{z\}$ not the exact depths of the locations of the boundaries between the various layers. This is again due to the fact that the current is so spread out and does not flow in a perfectly defined layer of, for example, exactly 3 cm thickness as it travels between

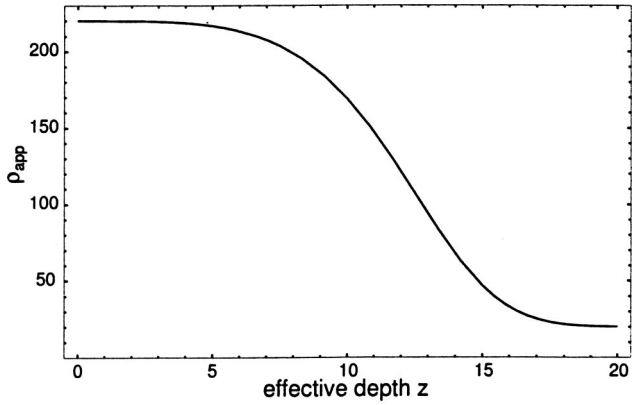

Fig. 4. Behavior of the apparent resistivity in a simple two-layer system. The apparent resistivity ρ_{app} is plotted vs the effective depth z of penetration of current into the subsurface. The units of ρ_{app} are Ω m.

the electrodes ***A*** and ***B***. Throughout this paper, all resistivities and all depths are effective resistivities and effective depths, respectively. True resistivity values and actual depths may be obtained from data acquired at the surface through various ''inversion methods'' in which information obtained at the surface is used to extract information about the subsurface. For the purposes of this paper, the use of effective depths and resistivities yields adequate information about the properties of the subsurface.

Determination of the effective depth of the boundary between the two layers may be performed using the so-called ''cumulative resistivity'' method. This method employs a plot of the sum of the apparent resistivities, $\Sigma\rho_{app}$, versus the effective depth.[8] The quantity $\Sigma\rho_{app}$ is referred to as the cumulative resistivity. In this method, the set of points plotted is determined by

$$\{(z,\Sigma\rho_{app})\}=\{(z_1,\rho_1),(z_2,\rho_1+\rho_2),(z_3,\rho_1+\rho_2+\rho_3),\ldots,(z_N,\rho_1+\cdots+\rho_N)\}. \quad (3)$$

There are two distinct linear sections to the curve in Fig. 5. The first section represents the summation of the constant

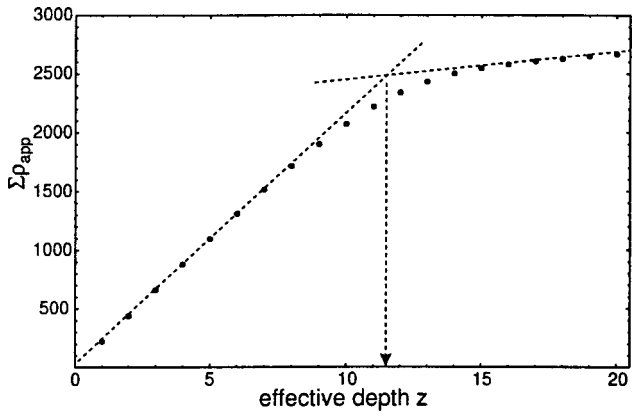

Fig. 5. Finding the depth to the boundary between the layers in a simple two-layer system using the method of cumulative resistivities. The cumulative resistivity, $\Sigma\rho_{app}$ is plotted vs the effective depth z. The points plotted are $\{(z,\Sigma\rho_{app})\}=\{(z_1,\rho_1),(z_2,\rho_1+\rho_2),(z_3,\rho_1+\rho_2+\rho_3),\ldots,(z_N,\rho_1+\cdots+\rho_N)\}$. The line drawn vertically downward from the intersection of the two straight segments on the graph indicates the effective depth to the boundary between the two layers.

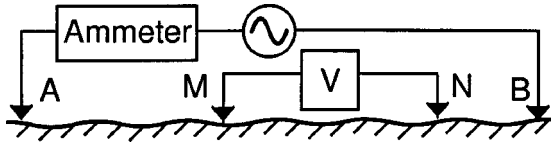

Fig. 6. General configuration of the four surface electrodes in linear resistivity surveys. Current is delivered through the electrodes *A* and *B*, and voltage readings are made with electrodes ***M*** and ***N***.

values of the resistivity of the upper layer. This yields a line of constant upward slope. The curve then deviates from this initial linear climb as the current encounters proportionally more of the lower layer. Eventually, the resistivity of the lower layer dominates and there is a new, smaller slope for the linear increase in the sum of the resistivities. In order to determine the depth of the boundary, straight lines are drawn along the two linear sections of the curve as shown in Fig. 5. A third straight line is drawn straight down from the intersection of the first two lines. The depth at ~11.5 m indicated by this third line is the depth of the boundary between the two layers.[8]

Figure 6 shows a general linear electrode configuration for a typical resistivity survey. All four electrodes are chosen to be in a straight line in the present work for simplicity. In general, the electrodes are not restricted to being collinear, although solving the electromagnetic field equations that accompany such arrays becomes more difficult.[10] The ac current source is in series with an ammeter, which measures the total current ***I*** going into the ground through the electrodes at points ***A*** and ***B***. A voltmeter attached to the two electrodes at points *M* and ***N*** measures the potential difference *V* between these points. By convention, the electrodes at the four surface points (*A, M, N, B*) are also named (*A, M, N, B*). The ratio (*V*/*I*) obtained is the apparent resistance for the entire subsurface. Section III will show how to obtain the appropriate geometric factor that, along with the apparent resistance, will construct the apparent resistivity ρ.

There are several ways in which the electrodes in Fig. 6 may be arranged, with the spacings chosen to match the needs of a particular survey site. Some of these arrangements are pictured in Fig. 7. Each of these electrode configurations has its own advantages and disadvantages, depending on the type of survey to be performed.[7]

The simplest of these arrays is the Wenner array, with the four electrodes equidistant from each other. The Wenner array is useful for resolving the differing resistivities of the subsurface layers straight down from the midpoint of the

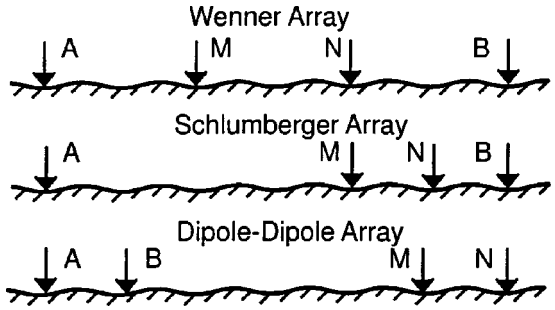

Fig. 7. Some common collinear electrode configurations for resistivity studies. The Schlumberger array is typically symmetric about a central point, but such symmetry is not required (shown here).

array. Vertical resolution of the various resistivities of the subsurface layers is achieved by increasing the common distance between the electrodes while maintaining the location of the center point of the array. Horizontal resolution is achieved by moving the electrodes laterally across the surface while maintaining a constant electrode separation.[7–10] The main drawback of the Wenner array is the large amount of work required to deploy the electrodes in the array. These must either be redeployed continuously in groups of four as the array is reconfigured for vertical or horizontal measurements, or else a great number of separate electrodes must be placed at the beginning of the survey and some sort of switching device used to activate four of the electrodes at a time. Commercial resistivity equipment employs a large number of electrodes and performs this switching automatically, while continuously reading and storing data.

The Wenner array is a highly symmetric form of the more general Schlumberger array. The math used to analyze the electrical signals from the Schlumberger array is the same as that for the Wenner array. The difference between the two arises through the geometric factor.[7–9] Less labor intensive than the deployment of either the Wenner or Schlumberger arrays, the dipole–dipole array is used where vertical depth penetration is paramount. The main drawbacks to the dipole–dipole arrangement are the lower vertical resolution obtained from its signal along with the relative lack of theoretical support for the analysis of the signal obtained with this array, especially when the four electrodes are not collinear.[7,10]

There are other electrode configurations in use, with each being chosen for its ability to resolve signals from a given source.[7] Each of the arrays discussed above must be analyzed mathematically in order to interpret real data from the field. The high degree of symmetry of the Wenner array makes it advantageous to study in an introductory geophysics class. This symmetry makes it easier for the students to visualize the current flow and equipotential lines. The mathematical derivations required to analyze the signal from the Wenner array are also more straightforward than those required to analyze the signals from the other arrays.

III. RESISTIVITY THEORY: MATHEMATICAL FORMULATION

Resistivity studies in geophysics may begin with the vector form of Ohm's law,[10]

$$\mathbf{J}=\sigma\mathbf{E}=\frac{\mathbf{1}}{\rho}\mathbf{E}=-\frac{\mathbf{1}}{\rho}\nabla\mathbf{V}. \tag{4}$$

In Eq. (4), **J** is the current density vector, **E** is the electric field vector measured in units of volts per meter, V is the electric potential in volts, σ is the conductivity measured in $(\Omega\,\mathrm{m})^{-1}$, and ρ is the resistivity measured in Ω m. The units of the current density are A/m^2 and should be brought to the attention of the students at the beginning of the derivation. The physical interpretation of the current density is that each component of **J** gives the amount of current flowing through each square meter of a two-dimensional surface perpendicular to the direction of flow of that component of **J**. For example, $\boldsymbol{J}_x$ indicates the number of amperes flowing in the $\boldsymbol{x}$ direction crossing each square meter of the $\boldsymbol{y}-\boldsymbol{z}$ plane.

Figure 2 shows a subsurface of uniform composition of infinite extent with one source and one sink electrode for the current. The current electrodes may be treated as point sources or sinks of spherically symmetric current flow in the half plane below the surface. The total current I flows away from or toward each electrode across the surface of a half sphere with area $\frac{1}{2}(4\pi r^2)$. Ohm's law for one electrode then has the simple form

$$\boldsymbol{J}=\frac{\boldsymbol{I}}{\frac{1}{2}(4\pi r^2)}=-\frac{1}{\rho}\frac{dV}{dr}. \tag{5}$$

For constant ρ, this first-order differential equation is readily integrated and yields

$$V(r)=\frac{\rho\boldsymbol{I}}{2\pi r} \tag{6}$$

for the potential a distance r from the electrode. In Eq. (6), I is the total current flowing from one current electrode to the other through the ground.

The electric potentials measured at M and $\boldsymbol{N}$ in the general linear array of Fig. 6 are superpositions of the potential of Eq. (6) due to each of the two source electrodes located at $\boldsymbol{A}$ and $\boldsymbol{B}$. With the distances between the electrodes given by AM, MB, etc., and $V=0$ infinitely far from the current source, the potentials at M and $\boldsymbol{N}$ are given by

$$V_{\boldsymbol{M}}=\frac{\rho\boldsymbol{I}}{2\pi}\left(\frac{1}{AM}-\frac{1}{MB}\right) \tag{7}$$

and

$$V_N=\frac{\rho I}{2\pi}\left(\frac{1}{\boldsymbol{A}N}-\frac{1}{\boldsymbol{N}B}\right). \tag{8}$$

The total potential difference between the electrodes $\boldsymbol{M}$ and $\boldsymbol{N}$ is thus

$$V_{\boldsymbol{M}N}=V_{\boldsymbol{M}}-V_N=\frac{\rho\boldsymbol{I}}{2\pi}\left[\left(\frac{1}{AM}-\frac{1}{MB}\right)-\left(\frac{1}{AN}-\frac{1}{\boldsymbol{N}B}\right)\right]. \tag{9}$$

This may be rearranged to yield

$$\rho=\frac{V_{MN}}{\boldsymbol{I}}\boldsymbol{K}, \tag{10}$$

where

$$K\equiv 2\pi\left[\left(\frac{1}{\boldsymbol{A}M}-\frac{1}{\boldsymbol{M}B}\right)-\left(\frac{1}{\boldsymbol{A}N}-\frac{1}{\boldsymbol{N}B}\right)\right] \tag{11}$$

is the "geometric factor" that will acquire a particular value for a given electrode spacing. For the Wenner array, all of the separations are equal to a constant value a and the Wenner geometric factor assumes the simple form $K=2\pi a$. Thus, the apparent resistivity for the Wenner array is

$$\rho_{\mathrm{Wenner}}=\left(\frac{V_{\boldsymbol{M}N}}{\boldsymbol{I}}\right)K=\left(\frac{V_{\boldsymbol{M}N}}{\boldsymbol{I}}\right)2\pi a. \tag{12}$$

Equation (12) is the first of the two main mathematical results of this section.

The resistivity of Eq. (12) is the apparent resistivity of the ground as measured by the surface electrodes. This value depends on the apparent resistance (V/I) and the geometric factor $\boldsymbol{K}$ that accounts for the electrode spacing. This is the same situation as encountered in the simple resistivity example of Eq. (2). The stratification of the subsurface is brought into the equation through the geometric factor K. As explained in Sec. II, the resistance that the current encounters is due more to the material that is closer to the surface than

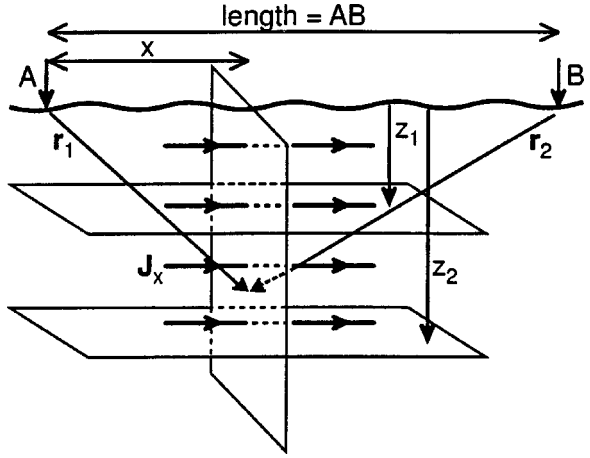

Fig. 8. Geometry for calculating the penetration depth of the current. The total electrode separation is *AB*. The *x*-component J_x of the total current density **J** is most relevant in this work. The vectors $\mathbf{r}_1$ and $\mathbf{r}_2$ go from the current electrodes ***A*** and ***B***, respectively, to a field point in the plane perpendicular to the line between the electrodes.

to the material that is further from the surface. This depth dependence of the measured resistivity needs to be evaluated mathematically in order to determine how much of the subsurface contributes to the effective resistivity measured by the Wenner array.

Equation (4) may be solved for the depth to which the current penetrates the subsurface material.[10] The generalized geometry within which Ohm's law will be solved is shown in Fig. 8. The horizontal component $\boldsymbol{J_x}$ of the current density is most relevant here. Due to the symmetry of the Wenner array, the deepest penetration for a given line of current in Fig. 8 will occur straight down from the center of the array where $\boldsymbol{x}=\boldsymbol{AB}/2$. A given portion I_x of the total current I will be flowing in the $\boldsymbol{x}$ direction between the two planes at depths z_1 and z_2. Finding a numerical value for I_x at $\boldsymbol{x}=AB/2$ will lead to a value for the effective penetration depth of the current.

With the potential for each electrode given by Eq. (6), the $\boldsymbol{x}$ component of the current density may be written as

$$\begin{aligned} J_{\boldsymbol{x}} &= -\frac{1}{\rho}\frac{dV}{dx} = -\frac{I}{2\pi}\frac{d}{dx}\left[\frac{1}{r_1}-\frac{1}{r_2}\right] \\ &= -\frac{I}{2\pi}\frac{d}{dx}[(\boldsymbol{x}^2+\boldsymbol{y}^2+z^2)^{-1/2} \\ &\quad -(\{\boldsymbol{x}-AB\}^2+\boldsymbol{y}^2+z^2)^{-1/2}] \\ &\equiv -\frac{I}{2\pi}\left[\frac{\boldsymbol{x}}{r_1^3}-\frac{\{\boldsymbol{x}-AB\}}{r_2^3}\right], \end{aligned} \tag{13}$$

where $r_1=(\boldsymbol{x}^2+\boldsymbol{y}^2+z^2)^{1/2}$, $r_2=([\boldsymbol{x}-\boldsymbol{AB}]^2+\boldsymbol{y}^2+z^2)^{1/2}$, and *AB* is the total separation between the two current electrodes. In the Wenner array, $\boldsymbol{x}=\boldsymbol{AB}/2$, $r_1=r_2\equiv r$, and Eq. (13) simplifies to

$$J_{\boldsymbol{x}}=\frac{\boldsymbol{I}}{2\pi}\left[\frac{\boldsymbol{AB}}{r^3}\right], \tag{14}$$

where $r=([AB/2]^2+\boldsymbol{y}^2+z^2)^{1/2}$. Equation (14) shows that more of the current travels nearer to the surface than further from the surface.

Equation (14) may now be used to calculate the fraction of the current that flows in the $\boldsymbol{x}$ direction through the subsurface below a given depth z_1. As mentioned above, J_x in Eq. (14) indicates the number of amperes flowing horizontally across every square meter of the $\boldsymbol{y}-z$ plane located under the surface. The infinitesimal amount of current $\delta \boldsymbol{I}_x$ flowing through an infinitesimal area $dy\,dz$ in the $\boldsymbol{y}-z$ plane is

$$\delta \boldsymbol{I}_x = J_x\,dy\,dz = \frac{I}{2\pi}\frac{\boldsymbol{AB}}{([\boldsymbol{AB}/2]^2+\boldsymbol{y}^2+z^2)^{3/2}}dy\,dz. \tag{15}$$

In order to get the total horizontal component of the current $\boldsymbol{I_x}$, Eq. (15) may be integrated over the $\boldsymbol{y}-z$ plane located at the midline of the Wenner array.[10] The total amount of current flowing through this plane between the depths $\boldsymbol{z}_1$ and z_2 is

$$\begin{aligned} \boldsymbol{I}_x &= \int_{z_1}^{z_2} dz \int_{-\infty}^{\infty} dy\, J_x = \frac{I}{2\pi}\int_{z_1}^{z_2} dz \int_{-\infty}^{\infty} \frac{\boldsymbol{AB}\,dy}{([\boldsymbol{AB}/2]^2+\boldsymbol{y}^2+\boldsymbol{z}^2)^{3/2}} \\ &= \frac{2I}{\pi}\left[\tan^{-1}\left(\frac{2\boldsymbol{z}_2}{\boldsymbol{AB}}\right)-\tan^{-1}\left(\frac{2z_1}{\boldsymbol{AB}}\right)\right]. \end{aligned} \tag{16}$$

The quantity I_x in Eq. (16) is that part of the total current I flowing in the $\boldsymbol{x}$ direction between the two depths z_1 and $\boldsymbol{z}_2$. This quantity is useful when information is needed about the subsurface in the vicinity of a certain depth. By taking the derivative with respect to ***AB***, it is straightforward to see that the fraction $\boldsymbol{I_x/I}$ has a broad peak at $\boldsymbol{AB}=2\sqrt{z_1 z_2}$. For example, in order to send the maximum current through the layer between the depths $\boldsymbol{z}_1=200\,\mathrm{m}$ and $z_2=310\,\mathrm{m}$, the outer electrodes should be spaced approximately 250 m apart.

Equation (16) also leads to the effective penetration depth of the current. If $\boldsymbol{z}_2\to\infty$ in Eq. (16), then z_1 delineates the boundary between a top layer and an infinitely deep lower layer. Thus, for $\boldsymbol{z}_2\to\infty$, $\boldsymbol{I_x}$ becomes

$$\boldsymbol{I_x}=I\left[1-\frac{2}{\pi}\tan^{-1}\left(\frac{2z_1}{\boldsymbol{AB}}\right)\right]. \tag{17}$$

The quantity $\boldsymbol{I_x}$ in Eq. (17) is now the amount of the total current I flowing through the ground below the depth z_1. Equation (17) shows mathematically what is indicated by Fig. 2: The further the outer current electrodes are spaced, the deeper the current penetrates into the ground, probing the subsurface composition to greater depths.

The idea that the spacing between ***A*** and ***B*** may now be used to quantify the penetration depth of the current is extremely important in resistivity surveys. Equation (17) indicates that half of the total current flows above z_1 and half of the total current flows below z_1 when $\boldsymbol{AB}=2\boldsymbol{z}_1$. The depth given by

$$\boldsymbol{z}=\boldsymbol{AB}/2 \tag{18}$$

acquires special meaning in resistivity surveys since it may now represent an "effective depth of penetration" of the current. This effective depth, in whatever mathematical form it appears, plays a major role in all resistivity surveys. It is fortunate that the effective depth *z* takes such a simple mathematical form in the Wenner array. While the expression for the effective depth assumes more mathematically complicated forms in other arrays, the Wenner expression actually gives a fairly good approximation for the effective penetra-

tion depth using these other arrays.[10] The effective depth $z = AB/2$ for the Wenner array, along with the apparent resistivity of Eq. (12) for the Wenner array, are the two main mathematical results of this section.

The effective depth may now be related to the system depicted in Fig. 4. When the effective depth reaches below the boundary between the two layers, the measured resistivity is determined more by the deeper material than the shallower material. The inflection point at the depth ~11.5 m shows where this crossover occurs and thus may also be used in very simple cases to determine the depth to the boundaries between the subsurface layers. Figure 5 shows this crossover as the nonlinear part of the curve between the two linear sections.

The effective depth is the depth over which resistivity information is averaged since the resistivity measured at the surface is the total resistivity of the entire subsurface through which the current is flowing. As stated previously, the numbers for the resistivity do not give the actual resistivity for the lower layers but an apparent resistivity. For example, if the actual resistivity of the upper layer in a two-layer system were 200 Ω m, and that of an infinitely thick lower layer were 5,000 Ω m, then the resistivity obtained when the effective depth z first penetrates into the lower layer is lowered from its true value due to the influence of the lower resistivity of the upper layer. Only when $z \gg d$, where d is the depth to the boundary, does the effective resistivity asymptotically approach 5,000 Ω m. In a system of more than two layers such as the one studied in Sec. V with this equipment, the apparent resistivity of the intermediate layer will be shown to be different from that of the other two layers. Yet the apparent resistivity, even though it appears to assume a stable value, will not be the actual resistivity due to the influence of the other two layers. Applying the procedure of finite element analysis[10] will construct the true resistivity values given the values of the apparent resistivities. The procedure of finite element analysis is discussed but not explored in depth in this course. Software accompanying commercial resistivity arrays typically performs this analysis for the user.

IV. RESISTIVITY APPARATUS

Taking resistivity data in the field requires an apparatus consisting of two basic parts as seen in Fig. 6. One part of the apparatus is a source for the current and should be capable of delivering power on the order of 100 W. The other part of the apparatus is a means of measuring the voltage at various points on the ground.

The apparatus pictured in Fig. 9 is easily constructed in the course of one afternoon since all components besides the electrodes themselves are ''plug and play.'' Most of the components were purchased directly from local stores that had nothing to do with geophysical equipment. The current source consists of a 12 V lawn tractor battery available at hardware stores. In order to convert this to the low frequency ac power, a 12-V dc to 115-V ac portable power converter[12] was attached to the battery using a car lighter socket with two battery clips.[13] The particular power converter used was capable of delivering 140 W continuous output power at 115 V ac. All connecting wires were 16 gauge braided speaker wire and were terminated on both ends with banana plugs. Alligator clips were added to the ends connecting to the electrodes. For the field surveys, large aluminum paper clamps were added to make the final connection to the large electrode easier. These clamps are available from office supply stores.

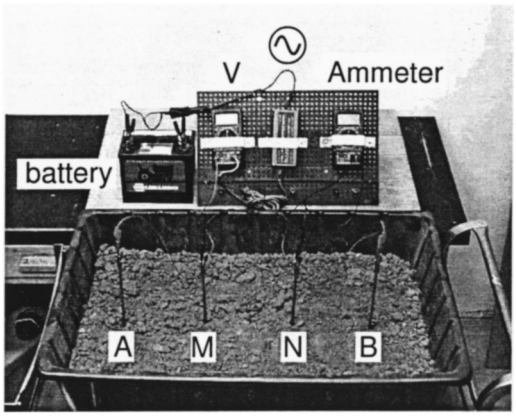

Fig. 9. ''Plug and play'' resistivity apparatus deployed in ~20 cm of soil in a bricklayer's mudpan. The four electrodes at *A*, *M*, *N* and *B* are 4 gauge copper wire. The voltmeter *V*, ac current source, and ammeter are all mounted on a perforated board with the battery adjacent. All connections are made with 16 gauge braided copper wire, banana plugs, and alligator clips and large aluminum paper clips.

The only modification to any piece of off-the-shelf equipment was the plug which connected the output of the power converter into the circuit. One end of a three-prong plug was plugged into the power converter. The other end was cut off, and the two live ac wires were terminated with banana plugs. The ground wire was not used and was covered with electrical tape for safety.

Different electrodes were used for the tabletop and the field measurements. The electrodes for the tabletop resistivity measurements were 10 cm lengths of 4 gauge copper wire. The electrodes for field studies were 60 cm sections cut from household use copper-coated steel lightning rods and sharpened to a point on one end. These rods are available from typical hardware stores.

The only specialized components in the apparatus were the two digital multimeters[14] that measure the total current flow and the voltage from the electrodes. These two multimeters combined with the power converter to comprise the bulk of the cost of the apparatus. The multimeters and the connections were all mounted on a piece of 30 cm × 60 cm perforated particle board using elastic straps. This open arrangement was chosen in order to keep all components and their connections in plain sight of students.

Table I. Tabletop resistivity data.

a (cm)	V (V)	I (mA)	z (cm)	ρ (Ω m)	$\Sigma\rho$ (Ω m)
1.5	20.3	70	2.3	27	27
3.0	9.6	45	4.5	40	68
5.0	9.8	65	7.5	47	120
8.0	7.6	46	12	83	200
10	9.9	56	15	110	310
12	7.8	38	18	160	460
15	6.5	25	23	250	710
18	6.5	18	27	410	1,100
20	5.9	17	30	440	1,600
24	6.2	12	36	780	2,300

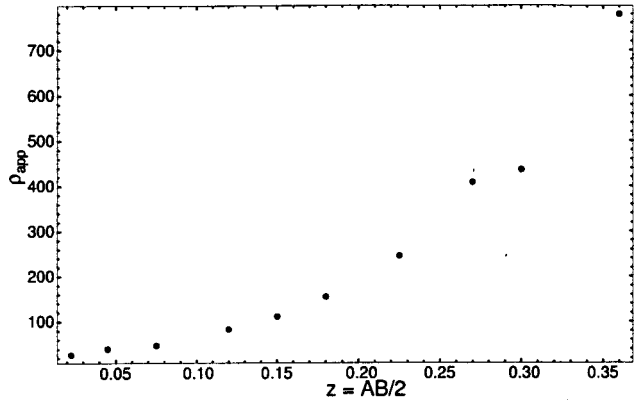

Fig. 10. Tabletop resistivity measurements. Apparent resistivity ρ_{app} vs effective depth $z=AB/2$. The actual depth of the soil in the pan is ~20 cm.

One concern when deploying the electrodes for surveys with both this array and commercial resistivity arrays is the consistency of electrical contact between the electrodes and the ground. For this reason, a small amount of slightly salty water or even water from a nearby stream should be poured on the base of the electrodes where they contact the ground. This water will ensure good contact between the electrodes and the ground. So long as the amount of water is small enough so as to not saturate the ground more than a couple of centimeters away from the electrodes, it will not interfere with the resistivity data.

V. RESULTS AND DISCUSSION

The apparatus was tested in a controlled setting by using a tabletop model for a two-layer system of known resistivities. This tabletop system was constructed using a bricklayer's ''mudpan'' (approximately 20 cm×60 cm×90 cm) filled to a depth of 20 cm with wet soil. Bringing the wet soil in has been most effective with the geology majors since it directly connects with their interests in real-world materials. The resistivity of wet soil should be around 10–100 Ω m,[7] while the resistivity of the underlying layer consisting of the bottom of the mudpan and the supporting table should effectively approach infinity. Measurements were made starting with a common electrode spacing of 1.5 cm. The final spacing of 24 cm ensured that the final effective depth of 36 cm was well below the depth of the soil in the container. The data and the results of the calculations are shown in Table I.

Table II. Floodplain resistivity data.

a (m)	V (V)	I (mA)	z (m)	ρ (Ω m)	$\Sigma\rho$ (Ω m)
0.10	10.72	24.2	0.15	280	280
0.20	4.60	25.3	0.30	230	510
0.30	3.60	32.9	0.45	210	710
0.50	1.54	33.9	0.75	140	860
1.0	0.61	39.2	1.50	98	950
1.5	0.43	37.6	2.25	110	1,100
2.0	0.34	35.9	3.00	120	1,200
3.0	0.25	46.8	4.50	100	1,300
4.0	0.21	35.4	6.00	150	1,400
6.0	0.49	36.3	9.00	510	1,900
8.0	0.48	36.3	12.0	670	2,600
12.0	0.62	39.5	18.0	1200	3,800

The resistivity of the wet soil is in the tens of Ω m as indicated by the first two data points in Table I. This is in agreement with the expected value for the wet soil.[7] Figure 10 shows the steady climb in the resistivity values as the probes are moved further apart. This reflects the probing of the tabletop array well into the near-infinite resistivity of the plastic of the container and into the wooden table below. Figure 11 shows a plot of the summation of the resistivities of the layers versus depth. The arrow drawn down from the intersection of the two straight segments of the graph indicates that the boundary between the upper layer of wet soil and the lower layer of the container and table was located at a depth of approximately 21 cm. This is in good agreement with the actual depth of 20 cm.

The classroom resistivity apparatus was also used to take resistivity data on two flat open fields using the Wenner electrode configuration. The first of these fields was a periodic floodplain on the Radford University campus adjacent to the New River. The local topography and the location of the river at the bottom of the valley allowed reasonable assumptions to be made prior to the survey about both the depth to the water table under the floodplain and the depth to the underlying bedrock. This would again allow the validity of the data obtained by the apparatus to be tested.

The data in Table II show that the subsurface of this field harbors at least three main layers. The resistivity of the topmost layer of soil is ~280 Ω m, a value characteristic of dry

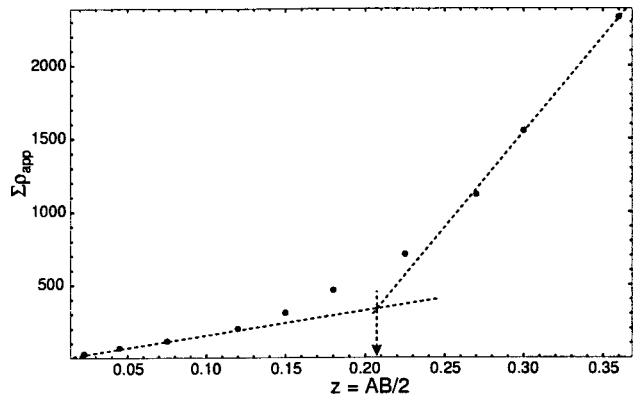

Fig. 11. Tabletop resistivity measurements. Cumulative apparent resistivity $\Sigma\rho_{app}$ vs effective depth $z=AB/2$. The depth to the boundary of this two-layer system is indicated by the line drawn vertically downward from the intersection of the two straight segments of the graph.

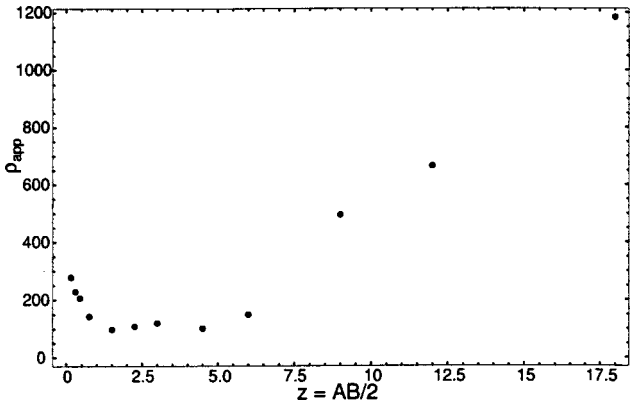

Fig. 12. Resistivity measurements in a floodplain. Apparent resistivity ρ_{app} vs effective depth $z=AB/2$.

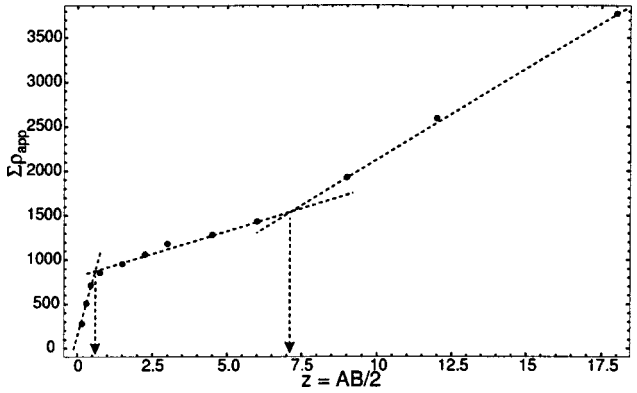

Fig. 13. Resistivity measurements in a floodplain. Cumulative apparent resistivity $\Sigma\rho_{app}$ vs effective depth $z=AB/2$. Finding the depths to the boundaries of a multilayer system.

topsoil.[7] As the effective depth z increases, the apparent resistivity decreases to $\sim 100\ \Omega\,\mathrm{m}$, indicating the presence of a layer with a higher water content. The apparent resistivity begins to increase when the effective depth is greater than 3.0 m, indicating the presence of a dry layer underlying the upper two layers. This three-layer structure is readily seen in Fig. 12. This figure shows the initial resistivity of the dry topsoil quickly falling with depth and reaching a steady value around $100\ \Omega\,\mathrm{m}$ when the effective depth is between 2 and 5 m. The apparent resistivity then begins to rise steadily with depth, revealing the presence of the third layer. Figure 13 indicates that the depths to the boundaries between these layers are approximately 0.5 and 7 m.

The three-layer structure indicated by Figs. 12 and 13 is consistent with a straightforward interpretation of the topography of the floodplain area. Figure 14 shows a cross section of the surface terrain of the floodplain. In Fig. 14, only vertical distances are drawn to scale due to space limitations. The shore of the New River begins a few meters to the north of the floodplain of the survey, with the bottom of the river lying ~ 4 m below the level of the survey field. The floodplain and the river are separated by an artificial levy. To the south of the floodplain are a series of progressively higher artificial terraces. These terraces follow the general rise in elevation of the valley to the south of the river. The New River is located in the bottom of the valley through which it flows, and, at the location of the survey, is approximately 70 m wide and 1 m deep.

Given the surface terrain near the river, reasonable conclusions concerning the subsurface could be drawn. The first conclusion is that the bottom of the river itself should not be far from the underlying bedrock through which the river has cut. In addition, the groundwater flowing from the higher elevations of the valley into the river would reasonably flow just below the surface and would follow the general slope of the terrain as it falls toward the river. The topsoil itself should have a relatively high resistivity since, after months of normal precipitation in the area, there was a two-week period of clear dry weather during which the water in the topsoil either evaporated or drained down to the level of the main groundwater flow. The three-layer structure of the subsurface indicated by this interpretation of the survey data is illustrated in Fig. 14.

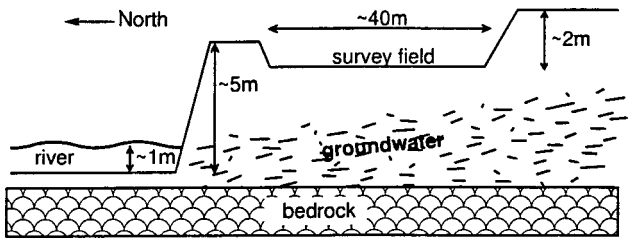

Fig. 14. Cross-sectional structure of the floodplain on the Radford University campus. Horizontal distances are not drawn to scale. The three layers of dry topsoil, saturated water table, and bedrock suggested by Fig. 13 are shown.

Table III. Sports field resistivity data.

a (m)	V (V)	I (mA)	z (m)	ρ (Ω m)	$\Sigma\rho$ (Ω m)
0.50	135	3.1	0.75	140	140
1.0	106	3.2	1.5	210	350
2.0	100	3.4	3.0	370	720
4.0	107	2.6	6.0	1,000	1,700
6.0	164	2.9	9.0	2,100	3,900
8.0	99.1	3.1	12	1,600	5,500
12	114	3.1	18	2,800	8,300
16	110	2.7	24	4,100	12,000
24	148	3.8	36	5,900	18,000
28	260	3.5	42	13,000	31,000
32	390	3.3	48	24,000	42,000

The third area surveyed with this apparatus was a sports field near the campus of a high school in the area. The survey area and depth to which the apparatus needed to penetrate were larger than the area and depths of the previous two surveys. This particular survey was attempted to determine the ability of this apparatus to conduct surveys of relatively large area and depth. The data set obtained from this field is shown in Table III. This survey was performed after a year in which the rainfall in the area was consistently below normal. The readings were obtained on a winter morning and the typical condensation was noted on the ground. There were no rivers near this field, unlike the floodplain of the survey described above.

Damp topsoil has a resistivity around $100\ \Omega\,\mathrm{m}$ while dry limestone, which would constitute the bedrock in the survey area, has a resistivity around $10^7\ \Omega\,\mathrm{m}$. The resistivities from Table III are graphed in Fig. 15. The transition from the lower resistivity of the overlying soil layers to the higher resistivity of the underlying bedrock is apparent. The resis-

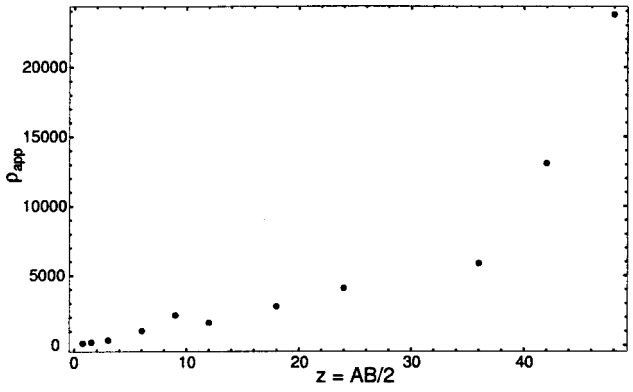

Fig. 15. Sports field resistivity measurements. Apparent resistivity ρ_{app} vs effective depth z.

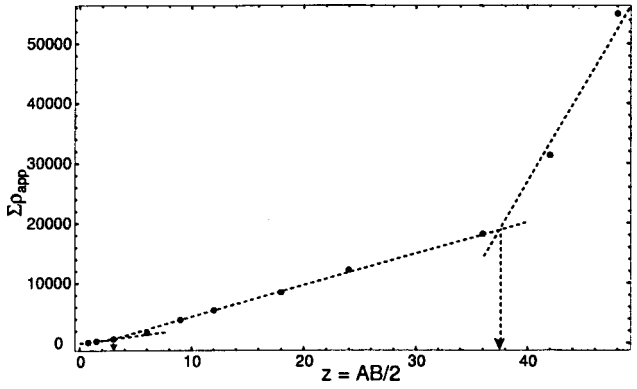

Fig. 16. Sports field resistivity measurements. Cumulative apparent resistivity $\Sigma\rho_{app}$ vs effective depth $z=AB/2$. The locations of the two boundaries are indicated by the two arrows drawn vertically downward from the intersections of the straight segments of the graph.

tivity of the soil layers starts at a value of 140 Ω m, consistent with damp topsoil. The resistivity steadily climbs from that value, reflecting the possible presence of a drier layer of fractured limestone beneath the topsoil. When the effective depth of the current crosses over into the region of bedrock, the resistivity values climb sharply. This climb seems to start abruptly at a depth of 35–40 m according to Fig. 15, but the depth to the bedrock is more appropriately determined from Fig. 16. Figure 16 shows the value in plotting $\Sigma\rho$ versus depth when adjacent layers have similar resistivity values. Figure 16 gives a stronger indication than Fig. 15 that there are three layers underlying this field.

This sports field was created by using topsoil fill dirt on top of fractured limestone in order to create a flat field in an area of sloping terrain. The data indicate the thickness of this topsoil fill to be ~3 m. Figure 16 also indicates that the depth to the bedrock underlying the field is approximately 38 m. This depth to bedrock is consistent with the construction history of buildings in the area.

The approach to introducing electrical resistivity methods in geophysics presented here has been successful in giving our students a firm grasp of the basic concepts in the field. While not as mathematically elegant as other approaches, geology students especially seem to remember the two basic equations dealing with the Wenner array. They are able to use Eqs. (12) and (18) as a framework within which to view the data obtained with commercial arrays. More than anything else, the effective depth allows them to visualize the probing of the subsurface with measurements taken at the surface.

The apparatus described here is capable of performing resistivity surveys that yield information about subsurface structure over a wide range of depths—from centimeters to tens of meters in the present work. The measurements obtained with this apparatus are valid, and are comparable with those that would be obtained by a much more expensive apparatus. The main drawback to this apparatus is the time required to properly site and connect the electrodes for field studies over large areas. Yet this constant redeployment makes students active participants in these surveys, and they are able to more clearly see the relationship between the spacing of the electrodes and the effective depth of the current. Again a perceived drawback becomes an advantage, just as the prohibitive cost of commercial resistivity arrays became an advantage in introducing the concepts of electrical resistivity surveys to students.

ACKNOWLEDGMENTS

The author would like to thank the faculty and students of the Southwest Virginia Governor's School for their help in data acquisition. This work was supported in part by a grant from the College of Arts and Sciences of Radford University.

[a]Electronic mail: rherman@radford.edu

[1]M. P. Silverman, "Self-directed learning: A heretical experiment in teaching physics," Am. J. Phys. **63** (6), 495–507 (1995).
[2]R. H. Parker and A. B. L. Whittles, "Introduction of special topics (geophysics) through the use of physics laboratory projects," Am. J. Phys. **38** (1), 65–67 (1970).
[3]G. M. Julian and A. M. Stueber, "Physicist+Geologist →Geophysics Course," Am. J. Phys. **42** (7), 556–559 (1974).
[4]R. A. Rudin, "Geophysics without geology," Am. J. Phys. **45** (6), 572–573 (1977).
[5]A. M. Conforto and F. Menzinger, "Proposal regarding a new general physics program for geologists," Am. J. Phys. **49** (5), 443–446 (1981).
[6]B. Avants, D. Soodak, and G. Ruppeiner, "Measuring the electrical conductivity of the earth," Am. J. Phys. **67** (7), 593–598 (1999).
[7]J. M. Reynolds, *An Introduction to Applied and Environmental Geophysics* (Wiley, New York, 1997).
[8]E. S. Robinson and C. Coruh, *Basic Exploration Geophysics* (Wiley, New York, 1988).
[9]H. R. Burger, *Exploration Geophysics of the Shallow Subsurface* (Prentice–Hall, Englewood Cliffs, NJ, 1992).
[10]W. M. Telford, L. P. Geldart, and R. E. Sheriff, *Applied Geophysics* (Cambridge U.P., Cambridge, 1990).
[11]J. D. Jackson, *Classical Electrodynamics* (Wiley, New York, 1975).
[12]Catalog No. 22-132B, Radio Shack, Division of Tandy Corporation, Fort Worth, TX 76102. Since this particular apparatus was first constructed, a newer and less expensive power converter has been purchased, the *MVP 300-W Power Inverter*, model A009014, available at most auto retail auto parts stores.
[13]Catalog No. 270-1527, Radio Shack, Division of Tandy Corporation, Fort Worth, TX 76102.
[14]Model 2706A, Jameco, Belmont, CA 94002.